J. Phys. Chem. A **2007,** *111,* 9291−9298 **9291**

Effects of Donor/Acceptor Strengths on the Multiphoton Absorption: An EOM-CCSD Correction Vector Study[†]

Yuanping Yi, Qingxu Li, Lingyun Zhu, and Zhigang Shuai*

Key Laboratory of Organic Solids, Beijing National Laboratory for Molecular Science (BNLMS), Institute of Chemistry, Chinese Academy of Sciences, 100080 Beijing, China

Received: April 23, 2007; In Final Form: May 31, 2007

We have developed a correction method (CV) to calculate the single- and multiphoton absorption (MPA) spectra of organic π-conjugated systems within the equation of motion coupled-cluster method with single and double excitations (EOM-CCSD). The effects of donor/acceptor strengths on the multiphoton absorption in a series of symmetrically substituted stilbene derivatives have been reinvestigated at both the ab initio and the semiempirical intermediate neglect of differential overlap (INDO) Hamiltonian levels. Both ab initio and INDO calculations show that the electron-donating or electron-withdrawing substituents lead to enhancements of two- and three-photon absorption cross sections, more pronounced for two-photon absorption than for three-photon absorption. The ab initio calculations usually produce larger excitation energies than the semiempirical, which lead to lower MPA cross sections.

Introduction

Multiphoton absorption (MPA) is a process that involves electronic excitation of a molecule induced by the simultaneous absorption of two or three photons. There is much experimental and theoretical interest in MPA because of numerous applications.[1−15] The advantage of MPA lies in two key features, (i) a longer excitation wavelength can be used so that it provides deeper penetration depths in absorbing media and (ii) a stronger spatial confinement can be achieved owing to the higher order dependence on the input light intensity. Apparently, three-photon absorption (3PA) is superior to two-photon absorption (2PA) in that respect. Design and synthesis of molecular materials possessing large MPA cross sections is the key to MPA applications. Accurately theoretical calculation and analysis of the origin of MPA may speed up this process.

At present, the time-dependent density functional theory (TDDFT) implemented in the response theory is available for calculating MPA properties.[16−20] Due to the lack of knowledge of exact exchange-correlation functional, one still has to test the applicability for different property determinations and to compare with other methods such as coupled-cluster theory (CC).[20] So far, the CC method is still one of the most accurate methods to consider the electron correlation for many-body systems. The equation of motion CC (EOM-CC) method[21−24] or the closely related coupled-cluster linear response (CCLR)[25−28] or symmetry-adapted-cluster configuration interaction (SAC-CI)[29−33] methods are the excited-state analogues of the highly accurate, efficient, and size-consistent CC method. The EOM-CC, specifically EOM-CCSD (single and double excitations), method has shown to be applicable for describing electronic excitations in conjugated systems.[34] With the excited states' information, one can calculate the MPA properties through the sum-over-states (SOS) method.[35] In this method, the MPA cross sections can be expressed as sums over transition dipole moment products, with transition energies as denominators. SOS is really accurate in the calculation of one-photon absorption (1PA) or sometimes 2PA properties. The tensor approach is an alternative method,[18,36,37] but it also involves SOS just with fewer folds of summation. However, in any case, it is extremely difficult to obtain all of the excited states' information for a medium or large size molecule, which will lead to uncontrolled truncation errors, especially for 3PA. One approach to overcome this difficulty is to use the correction vector (CV) method.[38−41] The CV method provides results which are exactly equal to those of the sum over all of the states within a given configuration space, but it only needs the ground-state properties, thus avoiding the impossible tasks of solving all of the excited states. Since Ramasesha and Soos suggested the CV technique in 1988,[38] the CV method has been implemented within the semiempirical SCI and SDCI Hamiltonian or PPP model Hamiltonian for the computation of first-, second-, or third-order nonlinear optical coefficients.[39,40] Recently, this method has been extended to the MRDCI framework for three-photon absorption properties.[41]

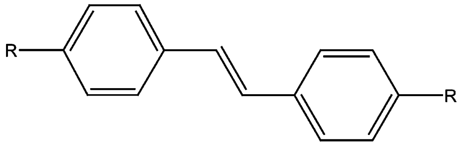

SB: R= -H, D1SB: R= -NH_2, A1SB: R= -CN,
BDPAS: R= -$N(Ph)_2$, D2SB: R= -$N(CH_3)_2$, A2SB: R= -NO_2.
D2SB in the experiments: R= -$N(Butyl)_2$

Figure 1. Chemical structures of the molecules studied in this work.

We note that following the pioneering work in CCLR by Koch and Jørgensen,[25] the nonlinear response based on the CC approach has been implemented to calculate the MPA properties.[20,42] Despite its great success in evaluating nonlinear optical response coefficients and multiphoton absorption cross sections at a fixed input frequency, there still exists challenge in predicting a full dynamic nonlinear spectrum due to the numerical difficulties in convergence. On another hand, our CV

[†] Part of the "Sheng Hsien Lin Festschrift".

* To whom correspondence should be addressed. E-mail: zgshuai@iccas.ac.cn.

10.1021/jp073137l CCC: $37.00

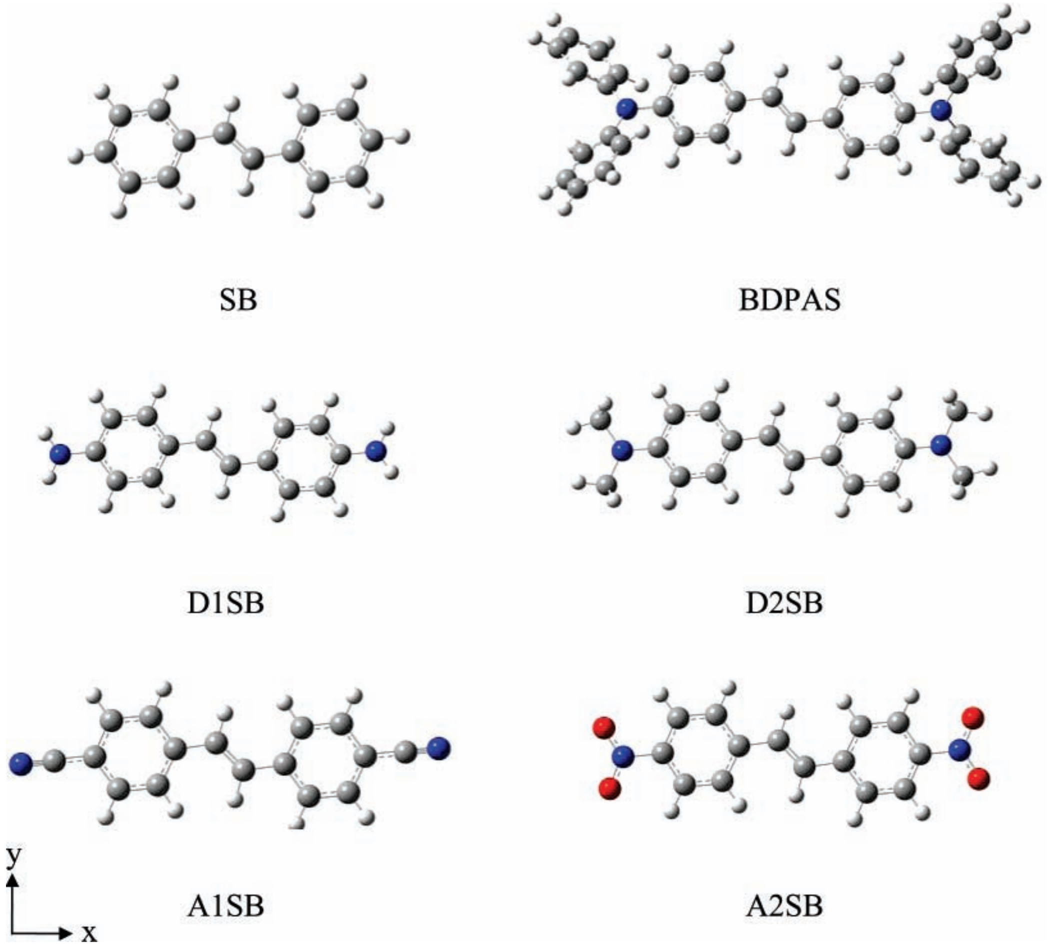

Figure 2. The optimized ground-state geometries of molecules. The *xyz* reference frame is also shown.

method is convergent even at resonant conditions for MPA,[41] thus providing more information than a single-frequency MPA cross section value because the experiments always give a measured MPA spectrum.

Recently, many molecules with the middle π bridges connecting to the side donors/acceptors (the so-called D−π−D/A−π−A systems) have been designed for efficient MPA materials. In this paper, we have examined the effects of donor/acceptor strengths on the 2PA and 3PA cross sections in a series of symmetrically substituted stilbene derivatives with the CV method within the EOM-CCSD approach at both ab initio and semiempirical INDO levels. Our calculations show that the substituents lead to obvious enhancement of 2PA cross sections but a relatively weak increase for 3PA cross sections and that the semiempirical INDO calculations, as well as the ab initio calculations, can give a proper picture for these properties.

Theoretical Methodology

For the closed-shell EOM-CCSD model, the ground state and the excited states can be written in a uniform expression[43]

$$|\mathrm{R}^m) = \sum_\mu \mathrm{R}_\mu^m \tau_\mu e^{\mathrm{T}}|0\rangle = e^{\mathrm{T}} \sum_\mu \mathrm{R}_\mu^m \tau_\mu |0\rangle = e^{\mathrm{T}} \sum_\mu \mathrm{R}_\mu^m |\mu\rangle \qquad (1)$$

In the above equation, $|0\rangle$ is Hartree−Fock (HF) ground-state determinant. T is the cluster operator which promotes electrons from the occupied to the virtual orbital space of the HF state, and truncated at single and double excitations, we obtain the excitation amplitudes by solving the ground-state CCSD equations proposed by Scuseria et al.;[44] τ_μ represents the excitation operators which are used to construct the spanned space $|\mu\rangle$, and specifically, τ_0 is the identity operator. R_μ^m is the expansion coefficient. The expansion coefficients are determined by the Schrödinger equation

$$\mathrm{H}|\mathrm{R}^m) = E^m|\mathrm{R}^m) \qquad (2)$$

where E^m is the energy of the mth state. As a special case, for the coupled-cluster ground state $|\mathrm{R}^0)$, all coefficients are $\mathrm{R}_\mu^0 = 0$ except $\mathrm{R}_0^0 = 1$. Substituting eq 1 into the above equation and then multiplying by $e^{-\mathrm{T}}$ on the left, we obtain the following equation

$$e^{-\mathrm{T}}\mathrm{H}e^{\mathrm{T}} \sum_\mu \mathrm{R}_\mu^m |\mu\rangle = E^m \sum_\mu \mathrm{R}_\mu^m |\mu\rangle \qquad (3)$$

The above equation can be written in a compact form as

$$\bar{\mathrm{H}}|\mathrm{R}^m\rangle = E^m|\mathrm{R}^m\rangle \qquad (4)$$

where

$$\bar{\mathrm{H}} = e^{-\mathrm{T}}\mathrm{H}e^{\mathrm{T}} \qquad (5)$$

$$|\mathrm{R}^m\rangle = \sum_\mu \mathrm{R}_\mu^m |\mu\rangle \qquad (6)$$

By combining eqs 1 and 5, $|\mathrm{R}^m)$ and $|\mathrm{R}^m\rangle$ are related by the following expression

$$|\mathrm{R}^m) = e^{\mathrm{T}}|\mathrm{R}^m\rangle \qquad (7)$$

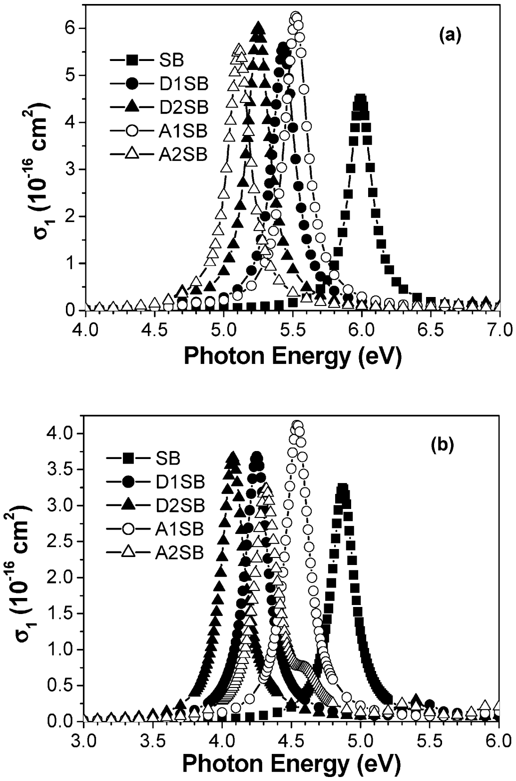

Figure 3. One-photon absorption spectrum (a) calculated by the ab initio method and (b) calculated by the semiempirical INDO method.

TABLE 1: The Calculated and Experimental 1PA Photon Energies (eV) at the First Peak of the Spectra

molecules	BDPAS	SB	D1SB	D2SB	A1SB	A2SB
exptl	3.20	4.18		3.32		
ab initio	4.87	5.99 5.84[a]	5.43	5.25	5.52	5.11
INDO	3.71	4.87	4.25	4.08	4.54	4.32

[a] Calculated with the 6-31G(d) basis set.

Similarly, the left vectors of the ground state and the excited states can be expressed as

$$(\mathrm{L}^m| = \langle \mathrm{L}^m|\mathrm{e}^{-\mathrm{T}} \tag{8}$$

where

$$\langle \mathrm{L}^m| = \sum_{\mu} \langle \mu|\mathrm{L}_{\mu}^{m} \tag{9}$$

The expansion coefficients of the left eigenvectors are determined by the following equation

$$\langle \mathrm{L}^m|\bar{\mathrm{H}} = \langle \mathrm{L}^m|E^m \tag{10}$$

Also, especially for the left vector of the ground state $(\mathrm{L}^0|$, the coefficient $\mathrm{L}_0^0 = 1$; the other coefficients are obtained by solving the linear equation, which is derived from eq 10. The ground and excited states are orthogonal and nearly normalized to the left eigenstates by using a biorthogonal basis.

The transition dipole moments between the ground state and the excited states can be expressed as

$$(\mathrm{L}^m|\bar{\vec{\mu}}i|\mathrm{R}^n) = \langle \mathrm{L}^m|\mathrm{e}^{-\mathrm{T}}\vec{\mu}_i\mathrm{e}^{\mathrm{T}}|\mathrm{R}^n\rangle = \langle \mathrm{L}^m|\bar{\vec{\mu}}_i|\mathrm{R}^n\rangle \tag{11}$$

where $\bar{\mu}_i = \mathrm{e}^{-\mathrm{T}}\vec{\mu}_i\mathrm{e}^{\mathrm{T}}$, and index i is the Cartesian coordinate.

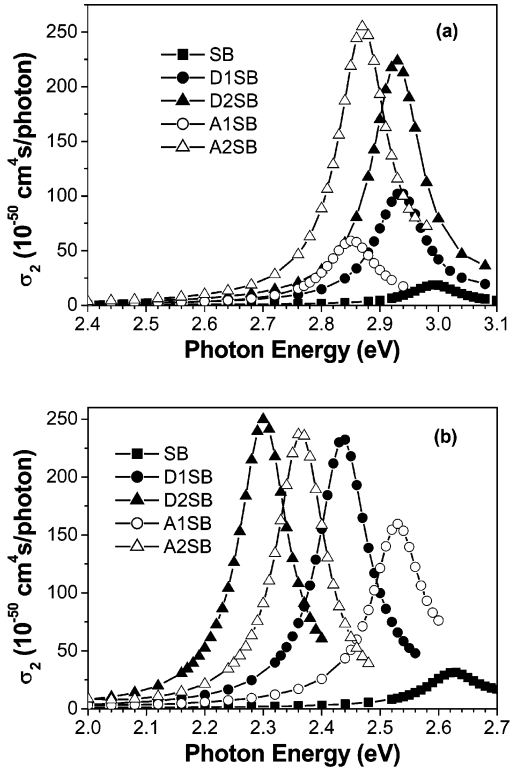

Figure 4. Two-photon absorption spectrum (a) calculated by the ab initio method and (b) calculated by the semiempirical INDO method.

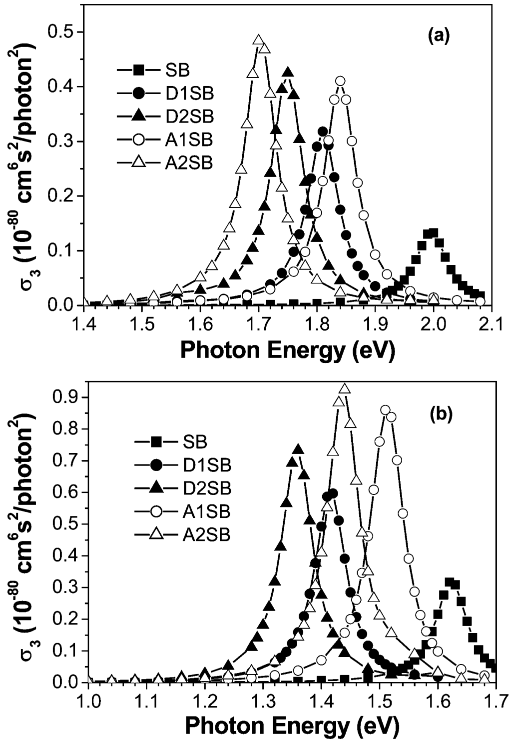

Figure 5. Three-photon absorption spectrum (a) calculated by the ab initio method and (b) calculated by the semiempirical INDO method.

From perturbation theory, the one-, two-, and three-photon absorption cross sections can be derived from the imaginary part of the first-, third-, and fifth-order polarizabilities, respectively.[45] These polarizabilities can be expressed in the SOS representation with the energies of the ground state and the excited states and the transition dipole moments between the states. For the first-order polarizability, it is expressed as[35]

$$\alpha_{ij} = \sum_{\mathrm{f}} \left[\frac{\langle \mathrm{L}^0 | \bar{\bar{\mu}}_i | \mathrm{R}^f \rangle \langle \mathrm{L}^f | \bar{\bar{\mu}}_j | \mathrm{R}^0 \rangle}{E^f - E^0 - \hbar\omega - i\Gamma} + \frac{\langle \mathrm{L}^0 | \bar{\bar{\mu}}_j | \mathrm{R}^f \rangle \langle \mathrm{L}^f | \bar{\bar{\mu}}_i | \mathrm{R}^0 \rangle}{E^f - \mathrm{E}^0 + \hbar\omega + i\Gamma} \right] \quad (12)$$

where $\hbar\omega$ is the input photon energy, Γ denotes the Lorentzian broadening factor (set to 0.1 eV in our calculations), and $\bar{\bar{\mu}}_\mathrm{i}$ is defined as

$$\bar{\bar{\mu}}_i = \bar{\mu}_i - \langle \mathrm{L}^0 | \bar{\mu}_i | \mathrm{R}^0 \rangle \quad (13)$$

From eq 12, to calculate the polarizabilities, we must make a truncation of the number of states involved in the summation because it is impossible to do a full diagonalization of the Hamiltonian matrix to obtain all states' information for a medium- or large-sized molecule. The uncontrollable truncation error can be eliminated using the CV method. For the first-order polarizability, it can be re-expressed as

$$\begin{aligned}\alpha_{ij} &= \sum_{f} \left[\frac{\langle \mathrm{L}^0 | \bar{\bar{\mu}}_i | \mathrm{R}^f \rangle \langle \mathrm{L}^f | \bar{\bar{\mu}}_j | \mathrm{R}^0 \rangle}{E^f - E^0 - (\hbar\omega + i\Gamma)} + \frac{\langle \mathrm{L}^0 | \bar{\bar{\mu}}_j | \mathrm{R}^f \rangle \langle \mathrm{L}^f | \bar{\bar{\mu}}_i | \mathrm{R}^0 \rangle}{E^f - E^0 + (\hbar\omega + i\Gamma)} \right] \\ &= \left\langle \mathrm{L}^0 \middle| \bar{\bar{\mu}}_i \middle| \frac{1}{\bar{\mathrm{H}} - E^0 - (\hbar\omega + i\Gamma)} \middle| \bar{\bar{\mu}}_j \middle| \mathrm{R}^0 \right\rangle + \\ &\qquad \left\langle \mathrm{L}^0 \middle| \bar{\bar{\mu}}_j \middle| \frac{1}{\bar{\mathrm{H}} - E^0 + (\hbar\omega + i\Gamma)} \middle| \bar{\bar{\mu}}_i \middle| \mathrm{R}^0 \right\rangle \\ &= \langle \mathrm{L}^0 | \bar{\bar{\mu}}_i | \phi_j^{(1)}(-\omega) \rangle + \langle \mathrm{L}^0 | \bar{\bar{\mu}}_j | \phi_i^{(1)}(\omega) \rangle \end{aligned} \quad (14)$$

where $|\phi_j^{(1)}(-\omega)\rangle$ and $|\phi_i^{(1)}(\omega)\rangle$ are the first-order correction vectors, which can be defined by the following equations[46,47]

$$[\bar{\mathrm{H}} - E^0 - (\hbar\omega + i\Gamma)] | \phi_j^{(1)}(-\omega) \rangle = | \bar{\bar{\mu}}_j | \mathrm{R}^0 \rangle \quad (15)$$

$$[\bar{\mathrm{H}} - E^0 + (\hbar\omega + i\Gamma)] | \phi_i^{(1)}(\omega) \rangle = | \bar{\bar{\mu}}_i | \mathrm{R}^0 \rangle \quad (16)$$

Similarly, from the SOS formulation of the third- and fifth-order polarizabilities, the second- and third-order correction vectors to the ground state, $|\phi_{ij}^{(2)}(\omega_1,\omega_2)\rangle$ and $|\phi_{ijk}^{(3)}(\omega_1,\omega_2,\omega_3)\rangle$, can be derived,[47] which obey

$$[\bar{\mathrm{H}} - E^0 + \hbar\omega_2 + i\Gamma_2] | \phi_{ij}^{(2)}(\omega_1,\omega_2) \rangle = \bar{\bar{\mu}}_j | \phi_i^{(1)}(\omega_1) \rangle \quad (17)$$

$$[\bar{\mathrm{H}} - E^0 + \hbar\omega_3 + i\Gamma_3] | \phi_{ijk}^{(3)}(\omega_1,\omega_2,\omega_3) \rangle = \bar{\bar{\mu}}_k | \phi_{ij}^{(2)}(\omega_1,\omega_2) \rangle \quad (18)$$

Since the transformed Hamiltonian matrix and the transformed transition dipole matrix $\bar{\bar{\mu}}_i$ are not symmetric, for the third- and fifth-order polarizabilities, the first- and second-order correction vectors to the left eigenvector of the ground state, $\langle \phi_i^{(1)}(\omega_1)|$ and $\langle \phi_{ij}^{(2)}(\omega_1,\omega_2)|$, should be calculated sequentially by solving the following equations

$$\langle \phi_i^{(1)}(\omega_1) | [\bar{\mathrm{H}} - E^0 + \hbar\omega_1 + i\Gamma_1] = \langle \mathrm{L}^0 | \bar{\bar{\mu}}_i \quad (19)$$

$$\langle \phi_{ij}^{(2)}(\omega_1,\omega_2) | [\bar{\mathrm{H}} - E^0 + \hbar\omega_2 + i\Gamma_2] = \langle \phi_i^{(1)}(\omega_1) | \bar{\bar{\mu}}_j \quad (20)$$

The linear algebraic equations (eqs 15−20) are solved efficiently by using a small matrix algorithm parallel to the iterative Davidson's diagonalization algorithm[41,48] for both positive and negative ω. In our program, the EOM-CCSD Hamiltonian matrix elements are not computed explicitly.

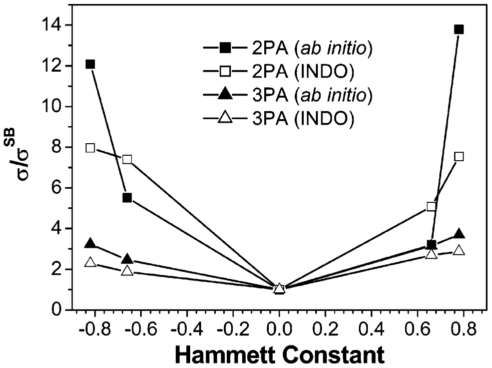

Figure 6. The ratios of the substituted molecules to SB for the simulated two- and three-photon absorption cross sections at the first peak.

During the iterations, we directly calculate the products of the Hamiltonian matrix and the added and renewed transformation vectors. This does not only save the memory but also reduces the computational magnitude. Since only one solution (not so many eigenvectors) is required, this allows calculation of even larger systems.

The first-, third-, and fifth-order polarizabilities (α, γ, ϵ) can be written in terms of the correction vectors as

$$\alpha_{ij}(\omega_\sigma;\omega_1) = \mathrm{P}_{ij} \langle \mathrm{L}^0 | \bar{\bar{\mu}}_i | \phi_j^{(1)}(-\omega_1) \rangle \quad (21)$$

$$\gamma_{ijkl}(\omega_\sigma;\omega_1,\omega_2,\omega_3) = \mathrm{P}_{ijkl} \langle \phi_i^{(1)}(-\omega_3) | \bar{\bar{\mu}}_j | \phi_{kl}^{(2)}(-\omega_1 - \omega_2, -\omega_1) \rangle \quad (22)$$

$$\epsilon_{ijklmn}(\omega_\sigma;\omega_1,\omega_2,\omega_3,\omega_4,\omega_5) = \mathrm{P}_{ijklmn} \langle \phi_{ij}^{(2)}(-\omega_1 - \omega_2, -\omega_1) | \bar{\bar{\mu}}_k | \phi_{lmn}^{(3)}(-\omega_3 - \omega_4 - \omega_5, -\omega_3 - \omega_4, -\omega_3) \rangle \quad (23)$$

where $\omega_\sigma = -\omega_1$ for α, $-(\omega_1 + \omega_2 + \omega_3)$ for γ, and $-(\omega_1 + \omega_2 + \omega_3 + \omega_4 + \omega_5)$ for ϵ; P is the permutation operator. The 1PA, 2PA, and 3PA cross sections are related to α if $\omega_1 = \omega$, γ if $\omega_1 = \omega_3 = \omega$ and $\omega_2 = -\omega$, and ϵ when $\omega_1 = \omega_3 = \omega_4 = \omega$ and $\omega_2 = \omega_5 = -\omega$. Since our studied molecules are quasi-one-dimensional systems, the MPA cross section is dominated by the main-direction component of the polarizability tensor. Thus, the 1PA, 2PA, and 3PA cross sections (σ_1, σ_2, and σ_3) can be expressed as

$$\sigma_1 = \frac{4\pi L^2}{\hbar nc} \bullet (\hbar\omega) \mathrm{Im}(\alpha_{xx}(-\omega;\omega)) \quad (24)$$

$$\sigma_2 = \frac{4\pi^2 L^4}{\hbar n^2 c^2} \bullet (\hbar\omega)^2 \mathrm{Im}(\gamma_{xxxx}(-\omega;\omega,-\omega,\omega)) \quad (25)$$

$$\sigma_3 = \frac{4\pi^3 L^6}{3\hbar n^3 c^3} \bullet (\hbar\omega)^3 \mathrm{Im}(\epsilon_{xxxxxx}(-\omega;\omega,-\omega,\omega,\omega,-\omega)) \quad (26)$$

Here, c is the speed of light in vacuum, n is a refractive index (set to 1.0 in the vacuum), and $L = (n^2+2)/3$ denotes a local field correction. When only taking the dominant resonant terms into account and making an orientational average, we can express σ_1, σ_2, and σ_3 as[37,49]

$$\sigma_1 = \frac{4\pi L^2}{3\hbar nc} \bullet (\hbar\omega) \bullet \mathrm{Im} \langle \mathrm{L}^0 | \bar{\bar{\mu}}_x | \phi_x^{(1)}(-\omega) \rangle \quad (27)$$

$$\sigma_2 = \frac{16\pi^2 L^4}{5\hbar n^2 c^2} \bullet (\hbar\omega)^2 \bullet \mathrm{Im} \langle \phi_x^{(1)}(-\omega) | \bar{\bar{\mu}}_x | \phi_{xx}^{(2)}(-\omega,-2\omega) \rangle \quad (28)$$

TABLE 2: The Calculated and Experimental 2PA Cross Sections and Photon Energies at the First Peak of the Spectra

molecules		BDPAS	SB	D1SB	D2SB	A1SB	A2SB
2PA cross section (10^{-50}cm^4 s/photon)	exptl	320	12		210		
	ab initio	508.0	18.5	102.0	223.6	59.1	255.1
			30.0[a]				
	INDO	156.5	31.4	232.3	249.8	159.5	236.6
2PA photon energy (eV)	exptl	1.85	2.41		2.05		
	ab initio	2.87	2.99	2.94	2.93	2.85	2.87
			3.04[a]				
	INDO	1.96	2.63	2.44	2.30	2.53	2.36

[a] Calculated with the 6-31G(d) basis set.

$$\sigma_3 = \frac{48\pi^3 L^6}{7\hbar n^3 c^3} \bullet (\hbar\omega)^3 \bullet \mathrm{Im}\langle \phi^{(2)}_{xx}(-\omega, -2\omega)|\bar{\bar{\mu}}_x|\phi^{(3)}_{xxx}(-\omega,-2\omega,-3\omega)\rangle \quad (29)$$

Computational Details

The chemical structures of the molecules studied in the present work are displayed in Figure 1. SB is the stilbene molecule. D1SB and D2SB are symmetrically donor-substituted SB derivatives. The acceptor-substituted compounds include A1SB and A2SB. We have also performed calculations on BDPAS to compare with the experimental results.[50a−b] For D2SB, the alkyl groups on the amino moieties in the experiments[50c] are replaced by methyl groups in our calculations. The ground-state geometries of the molecules are optimized at the density functional theory (DFT) level with the hybrid Becke three-parameter Lee−Yang−Parr (B3LYP) functionals and the 6-31G basis set, as implemented in the GAUSSIAN 03 package.[51]

From the optimized geometries, we did the EOM-CCSD calculations for the ground and excited states' properties at semiempirical and ab initio levels. For the semiempirical calculations, we have applied the EOM-CCSD approach coupled to the intermediate neglect of differential overlap (INDO) Hamiltonian.[52] The Mataga−Nishimoto potential[53] was used to describe the Coulomb repulsion terms. For the ab initio calculations, the Hartree−Fock self-consistent-field molecular orbitals (MOs) and dipole integrals as well as the two-electron integrals were derived directly from the GAMESS programs,[54] which were then used as the inputs to do our EOM-CCSD and CV calculations. The 6-31G basis set was chosen to construct the spanned space for the MOs. For both semiempirical and ab initio calculations, we kept all occupied and virtual π-conjugated molecular orbitals[55] in the active space.[56]

Results and Discussion

The optimized geometries of the calculated molecules are summarized in Figure 2. The molecules (the middle part of BDPAS) are taken to lie in the *xy*-plane, with the long axis oriented along the *x*-axis (Figure 2). Therefore, in this geometry, the dominant components are α_{xx}, γ_{xxxx}, and ϵ_{xxxxxx} for the first-, third-, and fifth-order polarizabilities. The electron-donating ability of the substituents increases from SB to D1SB to D2SB, as well as the electron-withdrawing ability from SB to A1SB to A2SB. It was shown previously that nonlinear optical properties of the compounds do correlate with the strengths of the substituents.[57,58]

The ab initio-calculated 1PA spectra of the molecules in the range of low photon energies are shown in Figure 3a. The electron-donating and electron-withdrawing substitutions have the same effects on the 1PA spectra. Compared with the spectrum of SB, the 1PA peak in the spectrum of the substituted systems is obviously red shifted with the increasing strength of the substituent, and σ_1 is enlarged slightly. The shape of the semiempirical INDO-polarized 1PA spectra (Figure 3b) is similar to that of the ab initio calculations, but the photon energies are about 1.0 eV lower than the ab initio results. In Table 1, we have presented the calculated and experimental[50] 1PA photon energies at the first peak. We find that the semiempirical results are in good agreement with the experiments, and the ab initio-calculated photon energies are somewhat overestimated for all studied molecules. This may be due to the inappropriate basis set.[59] However, we found that for 6-31G and 6-31G(d), the calculated MPA cross sections are very close each other; see Tables 1−3. This is in full agreement with Hurst et al. who found that for extended molecules, the basis effects for nonlinear optical response are much less than those for small molecules.[60]

Figure 4 shows the 2PA spectra of the studied molecules in the spectral range below the linear absorption. By replacing the hydrogen atoms of SB with donor/acceptor groups, σ_2 is enlarged drastically with the increased donor/acceptor strengths. This kind of phenomenon has also been demonstrated by experiments.[50c] From Table 2, we note that σ_2 measured by experiment is increased from 12 GM of SB to 210 GM of D2SB. Our results compare well with the experimental data. With the same basis set, the TDDFT-method-simulated σ_2 (218 GM) for the first peak is very close to the experimental result for D2SB,

TABLE 3: The Calculated and Experimental 3PA Cross Sections and Photon Energies at the First Peak of the Spectra and the Hammett Constants of the Donor/Acceptor Substituents for the Studied Molecules

molecules		BDPAS	SB	D1SB	D2SB	A1SB	A2SB
3PA cross section (10^{-80}cm^{6}s^2/photon^2)	exptl	0.5					
	ab initio	0.61	0.13	0.32	0.42	0.41	0.48
			0.11[a]				
	INDO	1.3	0.32	0.60	0.73	0.86	0.92
3PA photon energy (eV)	exptl	1.06					
	ab initio	1.62	2.00	1.81	1.75	1.84	1.70
			1.95[a]				
	INDO	1.23	1.62	1.42	1.36	1.51	1.44
Hammett constant			0.00	−0.66	−0.82	0.66	0.78

[a] Calculated with the 6-31G(d) basis set.

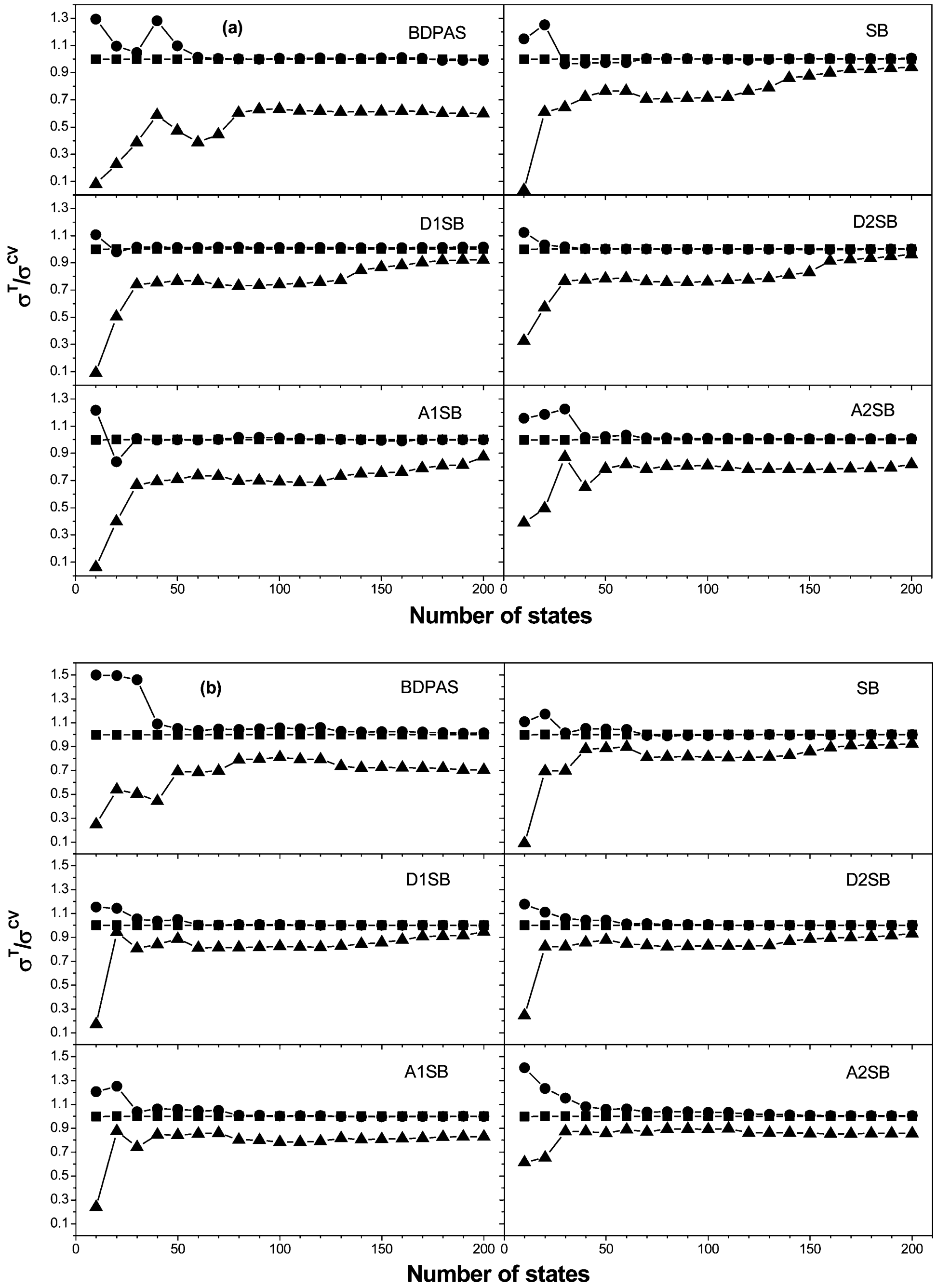

Figure 7. Evolution of the one-, two-, and three-photon absorption cross sections at the first peak obtained by the tensor approach with the number of intermediate states involved in the summation (a) calculated by the ab initio method and (b) calculated by the semiempirical INDO method. The square, circle, and triangle lines correspond to 1PA, 2PA, and 3PA, respectively.

but the σ_2 (186 GM) of SB is heavily overestimated.[16a] From Table 2, we find that the 2PA photon energies of the ab initio calculations are larger than the semiempirical INDO-method-calculated values. However, the semiempirical INDO method gives a bit larger σ_2 for SB, D1SB, and A1SB. The theoretical and experimental[50a] σ_2 and photon energies of BDPAS for the first peak are also presented in Table 2. Both the ab initio- and semiempirical INDO-method-calculated σ_2 deviate from the experimental data. The former is too large, while the latter is too small. The photon energies obtained through the semiempirical INDO calculations are closer to the experimental data than those obtained by the ab initio method.

The theoretical 3PA spectrum of SB and its substituted compounds is displayed in Figure 5. We have also calculated σ_3 for BDPAS (see Table 3). The simulated results compare well with the experimental data,[50b] though the photon energies of the ab initio calculations and σ_3 obtained by the semiempirical method are a bit overestimated. From Figure 5, we find that the 3PA spectrum is dominated by a single strong resonant peak in the spectral range where 1PA and 2PA are transparent. Because of the centrosymmetry in the studied molecules, the 1PA and 3PA peaks are associated with the same singlet excited state. This appears to be reflected in that the 3PA photon energy at the peak is about one-third of the 1PA energy (see Tables 1 and 3). Figure 6 displays the plot of the augment ratios of σ_2 and σ_3 for the first peak as a function of the Hammett constant of the substituents. The latter value reflects the electron-donating/withdrawing ability of the substituents. The constant of the donor/acceptor group is a negative/positive value. From Figure 6, we find that the ab initio and semiempirical INDO calculations give consistent enhancement of σ_3 by the donor/acceptor substitutions. However, the enhancement times for σ_3

are much less than those for σ_2. However, when the conjugated length of the investigated π systems is extended, σ_3 is increased much faster than σ_2, as our previous work indicated.[41] From Table 3, we find that the σ_3 values of the A−π−A molecules are larger than those of the D−π−D molecules, which have the same absolute values of the Hammett constant. This can be due to the elongated π systems by the substituted acceptor groups.

We have also calculated the MPA properties using the tensor approach. Figure 7 shows the evolution of MPA cross sections of the studied molecules for the first peak as a function of the number of intermediate states. Both the ab initio and the semiempirical results show that σ_1 obtained by the tensor approach is converged to the CV-method-calculated results with a few states. For 2PA, σ_2 is overestimated when it involves tens of states in the summation and then is converged well when it includes more than 100 states. However, σ_3 is always underestimated even if as many as 200 intermediate states are included. In one word, to obtain the converged results, more and more intermediate states are required with the increasing number of absorbed photons. Especially for 3PA, it is difficult to obtain enough excited states in the summation to calculate the converged σ_3. Here, the advantage of the CV method is obviously verified in that it directly gives the converged MPA spectra based only on the ground-state knowledge.

Conclusions

To conclude, we have applied the correction vector (CV) method to calculate the dynamic single and multiphoton absorption spectra for a series of donor/acceptor symmetrically substituted stilbene derivatives in the framework of the equation of motion coupled-cluster approach with single and double excitations (EOM-CCSD) coupled with the ab initio and the semiempirical intermediate neglect of differential overlap (INDO) Hamiltonian. The results show that the MPA spectra are red shifted through donor or acceptor substitution. The dependence of σ_3 on the strength of the donor or acceptor groups is monotonically increasing but weaker than that of σ_2. Compared with the ab initio results, the multiphoton absorption cross sections obtained by the semiempirical INDO method are usually overestimated, but the relatively small photon energies are closer to the experimental data. Also, the advantage of the ground-state-based CV method for the computation of converged MPA spectra is manifested.

Acknowledgment. This work is supported by NSFC (Grant Nos. 10425420, 20433070, 20421101, and 90503013) as well as the CNIC supercomputer center of the Chinese Academy of Sciences.

References and Notes

(1) Parthenopoulos, D. A; Rentzepis, P. M. *Science* **1990**, *245*, 843.

(2) Strickler, J. H.; Webb, W. W. *Opt. Lett.* **1991**, *16*, 1780.

(3) Dvornikov, A. S.; Rentzepis, P. M. *Opt. Commun.* **1995**, *119*, 341.

(4) Belfield, K. D.; Schafer, K. J. *Chem. Mater.* **2002**, *14*, 3656.

(5) Corredor, C. C.; Huang, Z.-L.; Belfield, K. D. *Adv. Mater.* **2006**, *18*, 2910.

(6) Denk, W.; Strickler, G. H.; Webb, W. W. *Science* **1990**, *248*, 73.

(7) Maruo, S.; Nakamura, O.; Kawata, S. *Opt. Lett.* **1997**, *22*, 132.

(8) Cumpston, B. H.; Ananthavel, S. P.; Barlow, S.; Dyer, D. L.; Ehrlich, J. E.; Erskine, L. L.; Heikel, A. A.; Kuebler, S. M.; Lee, I.-Y. S.; McCord-Maughon, D.; Qin, J. Q.; Rockel, H.; Rumi, M.; Wu, X. L.; Marder, S. R.; Perry, J. W. *Nature (London)* **1999**, *398*, 51.

(9) Kawata, S.; Sun, H.-B.; Tanaka, T.; Takada, K. *Nature (London)* **2001**, *412*, 697.

(10) Zhou, W. H.; Kuebler, S. M.; Braun, K. L.; Yu, T. Y.; Cammack, J. K.; Ober, C. K.; Perry, J. W.; Marder, S. R. *Science* **2002**, *296*, 1106.

(11) He, G. S.; Xu, G. C.; Prasad, P. N.; Reinhardt, B. A.; Bhatt, J. C.; Dillard, A. G. *Opt. Lett.* **1995**, *20*, 435.

(12) Perry, J. W.; Mansour, K.; Lee, I.-Y. S.; Wu, X. L.; Bedworth, P. V.; Chen, C. T.; Ng, D.; Marder, S. R.; Miles, P.; Wada, T.; Tian, M.; Sasabe, H. *Science* **1996**, *273*, 1533.

(13) Ehrlich, J. E.; Wu, X. L.; Lee, I.-Y. S.; Hu, Z. Y.; Rockel, H.; Marder, S. R.; Perry, J. W. *Opt. Lett.* **1997**, *22*, 1843.

(14) Fisher, W. G.; Partridge, W. P.; Dees, C.; Wachter, E. A. *Photochem. Photobiol.* **1997**, *66*, 141.

(15) He, G. S.; Markowicz, P. P.; Lin, T.-C.; Prasad, P. N. *Nature (London)* **2002**, *415*, 767.

(16) (a) Masunov, A.; Tretiak, S. *J. Phys. Chem. B* **2004**, *108*, 899. (b) Badaeva, E. A.; Timofeeva, T. V.; Masunov, A.; Tretiak, S. *J. Phys. Chem. A* **2005**, *109*, 7276.

(17) Angeli, C.; Bak, K. L.; Bakken, V.; Christiansen, O.; Cimiraglia, R.; Coriani, S.; Dahle, P.; Dalskov, E. K.; Enevoldsen, T.; Fernandez, B.; Hättig, C.; Hald, K.; Halkier, A.; Heiberg, H.; Helgaker, T.; Hettema, H.; Jensen, H. J. Aa.; Jonsson, D.; Jørgensen, P.; Kirpekar, S.; Klopper, W.; Kobayashi, R.; Koch, H.; Ligabue, A.; Lutnæs, O. B.; Mikkelsen, K. V.; Norman, P.; Olsen, J.; Packer, M. J.; Pedersen, T. B.; Rinkevicius, Z.; Rudberg, E.; Ruden, T. A.; Ruud, K.; Salek, P.; de Meras, A. S.; Saue, T.; Sauer, S. P. A.; Schimmelpfennig, B.; Sylvester-Hvid, K. O.; Taylor, P. R.; Vahtras, O.; Wilson, D. J.; Ågren, H. *DALTON, an Ab Initio Electronic Structure Program*, release 1.2; 2001; available from http://www.kjemi.uio.no/software/dalton/dalton.html.

(18) (a) Cronstrand, P.; Luo, Y.; Norman, P.; Ågren, H. *Chem. Phys. Lett.* **2003**, *375*, 233. (b) Cronstrand, P.; Jansik, B.; Jonsson, D.; Luo Y.; Ågren, H. *J. Chem. Phys.* **2004**, *121*, 9239. (c) Sałek, P.; Vahtras, O.; Guo, J.; Luo, Y.; Helgaker, T.; Ågren, H. *Chem. Phys. Lett.* **2003**, *374*, 446. (d) Sałek, P.; Ågren, H.; Baev, A.; Prasad, P. N. *J. Phys. Chem. A* **2005**, *109*, 11037.

(19) (a) Day, P. N.; Nguyen, K. A.; Pachter, R. *J. Phys. Chem. B* **2005**; *109*, 1803. (b) Day, P. N.; Nguyen, K. A.; Pachter, R. *J. Chem. Phys.* **2006**, *125*, 094103.

(20) (a) Paterson, M. J.; Christiansen, O.; Pawłowski, F.; Jørgensen, P.; Hättig, C.; Helgaker, T.; Sałek, P. *J. Chem. Phys.* **2006**, *124*, 054322. (b) Nielsen, C. B.; Rettrup, S.; Sauer S. P. A *J. Chem. Phys.* **2006**, *124*, 114108.

(21) Sekino, H.; Bartlett, R. J. *Int. J. Quantum Chem. Symp.* **1984**, *18*, 255.

(22) Geertsen, J.; Rittby, M.; Bartlett, R. J. *Chem. Phys. Lett.* **1989**, *164*, 57.

(23) Comeau, D. C.; Bartlett, R. J. *Chem. Phys. Lett.* **1993**, *207*, 414.

(24) Stanton, J. F.; Bartlett, R. J. *J. Chem. Phys.* **1993**, *98*, 7029.

(25) Koch, H.; Jørgensen, P. *J. Chem. Phys.* **1990**, *93*, 3333.

(26) Koch, H.; Jensen, H. J. Aa.; Jørgensen, P.; Helgaker, T. *J. Chem. Phys.* **1990**, *93*, 3345.

(27) Koch, H.; Kobayashi, R.; Jørgensen, P. *J. Chem. Phys.* **1994**, *100*, 4393.

(28) Christiansen, O.; Jørgensen, P.; Hättig, C. *Int. J. Quantum Chem.* **1998**, *68*, 1.

(29) Nakatsuji, H.; Hirao, K. *J. Chem. Phys.* **1978**, *68*, 2053.

(30) Nakatsuji, H. *Chem. Phys. Lett.* **1978**, *59*, 362.

(31) Nakatsuji, H. *Chem. Phys. Lett.* **1989**, *67*, 329.

(32) Nakatsuji, H. *Chem. Phys. Lett.* **1989**, *67*, 334.

(33) Nakatsuji, H. *Computational Chemistry, Reviews of Current Trends*; Leszczynski, J., Ed.; World Scientific: Singapore, 1996; Vol. 2, pp 62−124.

(34) (a) Shuai, Z.; Brédas, J. L. *Phys. Rev. B* **2000**, *62*, 15452. (b) Ye, A.; Shuai, Z.; Brédas, J. L. *Phys. Rev. B* **2002**, *65*, 045208. (c) Ye, A.; Shuai, Z.; Kwon, O.; Brédas, J. L.; Beljonne, D. *J. Chem. Phys.* **2004**, *121*, 5567. (d) Shuai, Z.; Li, Q.; Yi, Y. *J. Theor. Comput. Chem.* **2005**, *4*, 603.

(35) Orr, B. J.; Ward, J. F. *Mol. Phys.* **1971**, *20*, 513.

(36) Cronstrand, P.; Norman, P.; Luo, Y.; Ågren, H. *J. Chem. Phys.* **2004**, *121*, 2020.

(37) (a) Zhu, L.; Yang, X.; Yi, Y.; Xuan, P.; Shuai, Z.; Chen, D.; Zojer, E.; Brédas, J. L.; Beljonne, D. *J. Chem. Phys.* **2004**, *121*, 11060. (b) Zhu, L.; Yi, Y.; Shuai, Z.; Brédas, J. L.; Beljonne, D.; Zojer, E. *J. Chem. Phys.* **2006**, *125*, 044101.

(38) Ramasesha, S.; Soos, Z. G. *Chem. Phys. Lett.* **1988**, *153*, 171.

(39) (a) Ramasesha, S.; Shuai, Z.; Brédas, J. L. *Chem. Phys. Lett.* **1995**, *245*, 224. (b) Pati, S. K.; Ramasesha, S.; Shuai, Z.; Brédas, J. L. *Phys. Rev. B* **1999**, *59*, 14827. (c) Jha, P. C.; Das, M.; Ramasesha, S. *J. Phys. Chem. A* **2004**, *108*, 6279.

(40) (a) Shuai, Z.; Ramasesha, S.; Brédas, J. L. *Chem. Phys. Lett.* **1996**, *250*, 14. (b) Ray, P. C.; Leszczynski, J. *J. Phys. Chem. A* **2005**, *109*, 6689.

(41) Yi, Y.; Zhu, L.; Shuai, Z. *J. Chem. Phys.* **2006**, *125*, 164505.

(42) (a) Christiansen, O.; Gauss, J.; Stanton, J. F. *Chem. Phys. Lett.* **1998**, *292*, 437. (b) Gauss, J.; Christiansen, O.; Stanton, J. F. *Chem. Phys. Lett.* **1998**, *296*, 117. (c) Christiansen, O.; Gauss, J.; Stanton, J. F. *Chem. Phys. Lett.* **1999**, *305*, 147.

(43) Helgaker, T.; Jørgensen, P.; Olsen, J. *Molecular Electronic-Structure Theory*; John Wiley & Sons Ltd: Chichester, England, 2000; Chapter 13, pp 648−723.

(44) Scuseria, G. E.; Janssen, C. L.; Schaefer, H. F. *J. Chem. Phys.* **1988**, *89*, 7382.

(45) Peticolas, W. L. *Annu. Rev. Phys. Chem.* **1967**, *18*, 233.

(46) Stanton, J. F.; Bartlett, R. J. *J. Chem. Phys.* **1993**, *99*, 5718.

(47) (a) Hättig, C.; Christiansen, O.; Jørgensen, P. *J. Chem. Phys.* **1998**, *108*, 8331. Hättig, C.; Christiansen, O.; Jørgensen, P. *J. Chem. Phys.* **1998**, *108*, 8355.

(48) Ramasesha, S. *J. Comput. Chem.* **1990**, *11*, 545.

(49) (a) McClain, W. M. *J. Chem. Phys.* **1971**, 55, 2789. (b) McClain, W. M. *J. Chem. Phys.* **1972**, *57*, 2264. (c) Norman, P.; Cronstrand, P.; Ericsson, J. *Chem. Phys. Lett.* **2002**, *285*, 207.

(50) (a) Drobizhev, M.; Karotki, A.; Dzenis, Y.; Rebane, A.; Suo, Z.; Spangler, C. W. *J. Phys. Chem. B* **2003**, *107*, 7540. (b) Drobizhev, M.; Karotki, A.; Kruk, M.; Dzenis, Y.; Rebane, A.; Suo, Z.; Spangler, C. W. *J. Phys. Chem. B* **2004**, *108*, 4221. (c) Albota, M.; Beljonne, D.; Brédas, J. L.; Ehrlich, J. E.; Fu, J. Y.; Heikal, A. A.; Hess, S. E.; Kogej, T.; Levin, M. D.; Marder, S. R.; McCord-Maughon, D.; Perry, J. W.; Rockel, H.; Rumi, M.; Subramaniam, C.; Webb, W. W.; Wu, X. L.; Xu, C. *Science* **1998**, *281*, 1653.

(51) Frisch, M. J.; Trucks, G. W.; Schlegel, H. B.; Scuseria, G. E.; Robb, M. A.; Cheeseman, J. R.; Montgomery, J. A., Jr.; Vreven, T.; Kudin, K. N.; Burant, J. C.; Millam, J. M.; Iyengar, S. S.; Tomasi, J.; Barone, V.; Mennucci, B.; Cossi, M.; Scalmani, G.; Rega, N.; Petersson, G. A.; Nakatsuji, H.; Hada, M.; Ehara, M.; Toyota, K.; Fukuda, R.; Hasegawa, J.; Ishida, M.; Nakajima, T.; Honda, Y.; Kitao, O.; Nakai, H.; Klene, M.; Li, X.; Knox, J. E.; Hratchian, H. P.; Cross, J. B.; Bakken, V.; Adamo, C.; Jaramillo, J.; Gomperts, R.; Stratmann, R. E.; Yazyev, O.; Austin, A. J.; Cammi, R.; Pomelli, C.; Ochterski, J. W.; Ayala, P. Y.; Morokuma, K.; Voth, G. A.; Salvador, P.; Dannenberg, J. J.; Zakrzewski, V. G.; Dapprich, S.; Daniels, A. D.; Strain, M. C.; Farkas, O.; Malick, D. K.; Rabuck, A. D.; Raghavachari, K.; Foresman, J. B.; Ortiz, J. V.; Cui, Q.; Baboul, A. G.; Clifford, S.; Cioslowski, J.; Stefanov, B. B.; Liu, G.; Liashenko, A.; Piskorz, P.; Komaromi, I.; Martin, R. L.; Fox, D. J.; Keith, T.; Al-Laham, M. A.; Peng, C. Y.; Nanayakkara, A.; Challacombe, M.; Gill, P. M. W.; Johnson, B.; Chen, W.; Wong, M. W.; Gonzalez, C.; Pople, J. A. *Gaussian 03*; Gaussian, Inc.: Pittsburgh, PA, 2004.

(52) Ridley, J.; Zerner, M. C. *Theor. Chim. Acta* **1973**, *32*, 111.

(53) (a) Mataga, N.; Nishimoto, K. Z. *Phys. Chem.* **1957**, *12*, 35. (b) Mataga, N.; Nishimoto, K. Z. *Phys. Chem.* **1957**, *13*, 140.

(54) (a) Schmidt, M. W.; Baldridge, K. K.; Boatz, J. A.; Elbert, S. T.; Gordon, M. S.; Jensen, J. J.; Koseki, S.; Matsunaga, N.; Nguyen, K. A.; Su, S.; Windus, T. L.; Dupuis, M.; Montgomery J. A. *J. Comput. Chem.* **1993**, *14*, 1347. (b) Gordon, M. S.; Schmidt, M. W. *Theory and Applications of Computational Chemistry*, *the First Forty Years*; Dykstra, C. E., Frenking, G., Kim, K. S., Scuseria, G. E., Eds.; Elsevier, Amsterdam, The Netherlands, 2005; pp 1167−1189.

(55) We first project the *p*th molecular orbital (C_μ^p) to the direction perpendicular to the conjugation plane, denoted as Π_μ^p. This molecular orbital *p* can be regarded as a π orbital if

$$\sum_\mu (\Pi_\mu^p)^2 \Big/ \sum_\mu (C_\mu^p)^2 \geq 0.6$$

(56) Albert, I. D. L.; Morley, J. O.; Pugh, D. *J. Chem. Phys.* **1995**, *102*, 237.

(57) Sastre, A.; Díaz-García, M. A.; del Rey, B.; Dhenaut, C.; Zyss, J.; Ledoux, I.; Agulló-López, F.; Torres, T. *J. Phys. Chem. A* **1997**, *101*, 9773.

(58) Drobizhev, M.; Makarov, N. S.; Stepanenko, Y.; Rebane, A. *J. Chem. Phys.* **2006**, *124*, 224701.

(59) Pedersen, T. B.; Sánchez de Merás, A. M. J.; Koch, H. *J. Chem. Phys.* **2004**, *120*, 8887.

(60) Hurst, G. J. B.; Dupuis, M.; Clementi, E. *J. Chem. Phys*. **1988**, *89*, 385.